

SEBA: Sample-Efficient Black-Box Attacks on Visual Reinforcement Learning

Tairan Huang Yulin Jin Junxu Liu Qingqing Ye Haibo Hu
The Hong Kong Polytechnic University
Hong Kong, China

{tairan.huang, yulin.jin}@connect.polyu.hk
{junxu.liu, qqing.ye, haibo.hu}@polyu.edu.hk

Abstract

Visual reinforcement learning has achieved remarkable progress in visual control and robotics, but its vulnerability to adversarial perturbations remains underexplored. Most existing black-box attacks focus on vector-based or discrete-action RL, and their effectiveness on image-based continuous control is limited by the large action space and excessive environment queries. We propose **SEBA**, a sample-efficient framework for black-box adversarial attacks on visual RL agents. SEBA integrates a shadow Q model that estimates cumulative rewards under adversarial conditions, a generative adversarial network that produces visually imperceptible perturbations, and a world model that simulates environment dynamics to reduce real-world queries. Through a two-stage iterative training procedure that alternates between learning the shadow model and refining the generator, SEBA achieves strong attack performance while maintaining efficiency. Experiments on MuJoCo and Atari benchmarks show that SEBA significantly reduces cumulative rewards, preserves visual fidelity, and greatly decreases environment interactions compared to prior black-box and white-box methods. Our code is provided in the supplementary material.

1. Introduction

Reinforcement learning (RL) from visual observations [4, 28] has become a cornerstone of embodied intelligence, powering applications in robotic manipulation [21], autonomous navigation [18], and visual control [16]. Building on the foundation of deep reinforcement learning [23, 27], visual RL enables agents to learn control policies directly from raw pixel inputs and operate effectively in high-dimensional, dynamic environments without relying on hand-crafted state representations. However, this reliance on visual perception also makes such systems vulnerable to small, carefully crafted perturbations known as *adversarial attacks* [10–13, 25, 33], which can cause severe degrada-

tion or even catastrophic failures in control and decision-making. Understanding and improving the robustness of visual RL agents is therefore critical for ensuring the safe deployment of learning-based autonomous systems in real-world environments.

Despite the growing attention to adversarial robustness in RL, existing studies remain limited in scope. Most prior works focus on *vector-based* RL [33] or *discrete-action* visual RL (e.g., Atari) [25, 32], where the environment state is either low-dimensional or where the policy resembles a classifier [33]. In contrast, *continuous-action* visual RL presents a far more challenging setting: the action space is infinite, the observation space is high-dimensional, and perturbations can affect long-horizon dynamics in complex ways. To date, there has been little exploration of how to perform effective and efficient adversarial attacks in this setting, especially under the practical constraint of **black-box access**, where the attacker cannot observe gradients or internal model parameters.

Designing such an attack introduces multiple challenges. First, the black-box constraint prevents direct gradient computation, requiring the attacker to infer vulnerabilities purely from external observations of state, action, and reward. Second, naively estimating attack gradients via repeated environment queries is prohibitively expensive, as each rollout in RL entails costly sequential interaction. Third, the attacker must balance three competing objectives: attack *strength* (reward degradation), *imperceptibility* (maintaining visual realism), and *sample efficiency* (minimizing query cost). Achieving all three simultaneously demands a principled framework that can model long-term reward effects, produce realistic perturbations, and reduce dependence on real environment feedback.

To address these challenges, we propose **SEBA** (*Sample-Efficient Black-box Attacks*), a novel framework for efficient adversarial perturbation generation in visual RL with black-box access. SEBA integrates four key components: a *shadow Q model* that estimates cumulative reward under perturbations, a *GAN module* for perceptual realism, a *two-*

stage alternating training scheme to stabilize optimization, and a *world model module* that improves sample efficiency via synthetic rollouts.

We conduct extensive experiments to validate SEBA. On **MuJoCo** visual control tasks, SEBA surpasses all existing white-box and black-box baselines, achieving state-of-the-art performance in terms of reward degradation, visual imperceptibility, and query efficiency. On **Atari** benchmarks, SEBA remains highly competitive, outperforming most white-box methods and second only to PA-AD, while maintaining substantially lower query costs. We further demonstrate SEBA’s ability to perform *targeted* attacks, precisely steering specific action dimensions toward desired outcomes. These results collectively highlight SEBA’s effectiveness, efficiency, and subtlety across diverse reinforcement learning domains.

Contributions. This work makes the following key contributions:

- We tackle the open challenge of performing *sample-efficient black-box adversarial attacks* on visual reinforcement learning agents, where direct gradient access and extensive environment interaction are both infeasible.
- We propose **SEBA**, a two-stage framework that combines a shadow Q model, a GAN-based perturbation generator, and a learned world model. The shadow Q model supplies Q -based guidance without accessing the victim’s internals, while the world model generates synthetic rollouts to reduce real-environment queries.
- Comprehensive experiments across both continuous-control (**MuJoCo**) and discrete-action (**Atari**) domains show that SEBA achieves stronger attack effectiveness, higher visual imperceptibility, and greater query efficiency than existing white-box and black-box methods.

SEBA offers a principled and practical framework for efficient visual attacks in reinforcement learning, advancing the state of the art toward realistic, deployable black-box adversarial evaluation in embodied AI systems.

2. Related Work

2.1. Visual Reinforcement Learning

Visual RL trains agents directly from raw image observations. To handle high-dimensional inputs, it relies on representation learning that encodes images into compact latent features. Existing methods are mainly divided into prediction-based and image-based approaches.

Prediction-based algorithms [8, 34] facilitate Visual RL agent training by constructing a latent dynamics model. For example, IRIS [22] integrates a discrete autoencoder with an autoregressive Transformer to learn a world model. Additionally, [26] introduces a bidirectional self-predictive learning algorithm, and DeepMDP [5] trains the latent space model through the prediction of reward and subse-

quent latent states.

Image-based algorithms leverage computer vision techniques to train encoders. DrQ [30] trains encoders directly with data augmentation, removing the need for auxiliary tasks. CURL [14] formulates a contrastive learning objective using query-key pairs. SAC-AE [31] enhances training with deterministic autoencoders and reconstruction loss. ALIX [3] modifies latent representations by mixing components with their neighbors in the feature map.

2.2. Adversarial Attack on Reinforcement Learning

Adversarial attacks on reinforcement learning aim to craft perturbations that mislead the victim agent and significantly degrade its performance. Prior studies have explored various attack strategies. [24] applies gradient-based methods to manipulate agent behavior. SA-MDP [32] proposes critic-based and maximal-action-difference attacks. OPTIMAL [33] defines the adversary’s reward as the negative of the victim’s return, allowing the attacker to learn through reinforcement learning. PA-AD [25] combines an RL-based director with a non-RL actor, forming a white-box attack. [17] introduces Maximum Cost and Maximum Reward attackers. SAIA [29] employs imitation learning for targeted attacks, while [20] adopts a meta-MDP framework to model interactions between the attacker, victim, and environment.

Most existing attacks focus on agents with vector-based states. Although SA-MDP [32] and PA-AD [25] have been extended to visual RL, they are limited to discrete-action Atari environments, where the policy network acts like a classifier [33]. To our knowledge, this is the first work to investigate visual RL attacks in continuous control tasks, a more challenging setting.

3. Method: SEBA

In this section, we present the proposed **SEBA** (Sample-Efficient Black-box Attack) framework for visual reinforcement learning. We first describe the overall problem formulation and adversarial setting (§3.1). Then, we introduce the *shadow Q model* that provides black-box guidance (§3.2) and the GAN-based perturbation module for generating imperceptible yet effective attacks (§3.3). Next, we detail the two-stage alternating optimization strategy (§3.4) and the incorporation of a learned world model to improve query efficiency (§3.5). Finally, we summarize the overall training pipeline and algorithms (§3.6). An overview of the complete procedure is shown in Fig. 1.

3.1. Problem Setup

Let $\mathcal{M} = \langle \mathcal{S}, \mathcal{A}, p, r, \gamma \rangle$ be an MDP with image observations $s \in [0, 1]^{C \times H \times W}$ and continuous actions $a \in \mathcal{A} \subset \mathbb{R}^d$. A victim policy $\pi(a | s)$ is given in *black-box* form: we may query π to obtain actions but cannot access internals or gradients. The attacker outputs a bounded perturbation

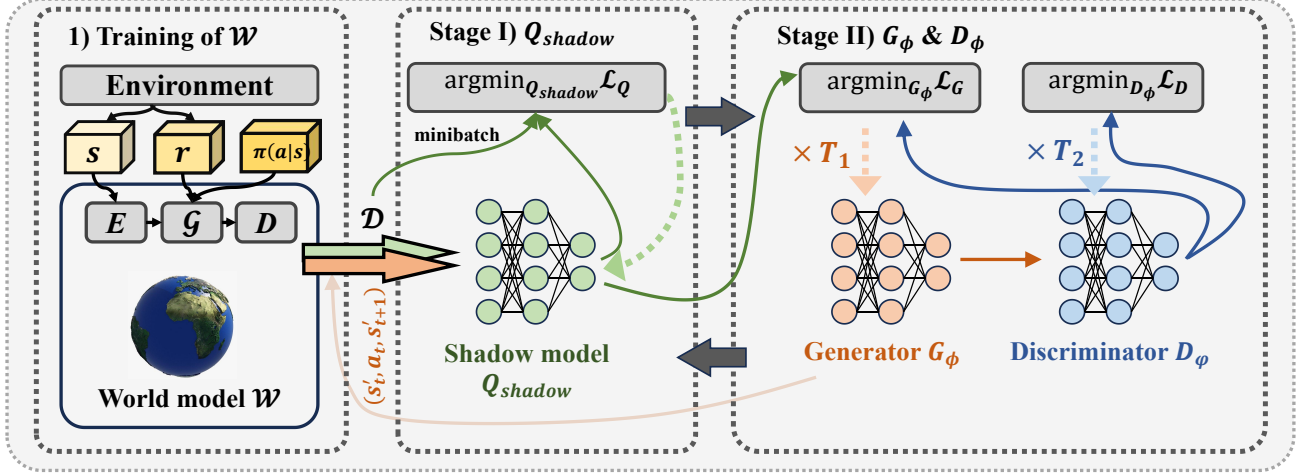


Figure 1. **SEBA overview.** The world model is first trained to predict visual dynamics and generate synthetic rollouts. SEBA then alternates between updating the shadow critic on perturbed states and optimizing the GAN.

$\delta = \text{clip}(G_\phi(s), -\epsilon, \epsilon)$ and forms $s' = \text{clip}(s + \delta, 0, 1)$. The attack objective is to minimize the discounted return of the victim:

$$\min_{\phi} \mathbb{E} \left[\sum_{t=0}^{\infty} \gamma^t r(s'_t, a_t) \right], \quad a_t \sim \pi(\cdot | s'_t). \quad (1)$$

3.2. Shadow Model Training

The shadow critic Q_{shadow} serves as a differentiable surrogate for the victim policy, estimating its expected cumulative reward under adversarial perturbations. This model provides the attacker’s optimization signal in a fully black-box setting.

During training, the generator G_ϕ adds bounded perturbations δ_t to clean observations s_t to form adversarial states $s'_t = s_t + \delta_t$. The victim policy $\pi(a|s'_t)$ is then executed to produce the corresponding action a_t , which interacts with the environment to produce rewards r_t and next states s_{t+1} . The process repeats to yield transition tuples $(s'_t, a_t, r_t, s'_{t+1}, \text{done}_t)$ stored in a replay buffer for updating Q_{shadow} .

The shadow model is optimized via the temporal-difference (TD) objective:

$$\begin{aligned} \mathcal{L}_Q &= \frac{1}{2} \mathbb{E} \left[(Q_{\text{shadow}}(s'_t, a_t) - y_t)^2 \right], \\ y_t &= r_t + \gamma \mathbb{E}_{a \sim \pi(\cdot | s'_{t+1})} [Q_{\text{shadow}}(s'_{t+1}, a)], \end{aligned} \quad (2)$$

where r_t is the immediate reward and γ is the discount factor. The victim policy π is executed only to produce actions, without accessing its gradients or internal parameters.

To enhance training efficiency, SEBA alternates between **real-environment updates** and **world-model updates**. During Q_{shadow} training, both real and synthetic transitions are utilized, ensuring accurate supervision from real

rollouts while leveraging the world model to reduce interaction cost.

3.3. GAN-based Perturbation Generation

To generate effective yet visually imperceptible perturbations, SEBA employs a generative adversarial framework composed of a generator G_ϕ and a discriminator D_ψ . The generator produces bounded pixel perturbations, while the discriminator enforces realism by distinguishing clean states from their adversarial counterparts.

Given a batch of observations $\{s_k\}_{k=1}^B$, adversarial states are formed as $s'_k = \text{clip}(s_k + G_\phi(s_k), 0, 1)$. The victim policy $\pi(a|s'_k)$ is then executed to obtain corresponding actions a_k . These interactions can be obtained from either the real environment or the learned world model (Sec. 3.5), depending on whether training uses real or simulated experience.

The discriminator and generator are optimized with opposing objectives:

$$\begin{aligned} \mathcal{L}_D &= -\frac{1}{B} \sum_{k=1}^B [\log D_\psi(s_k) + \log(1 - D_\psi(s'_k))], \\ \mathcal{L}_G &= -\frac{1}{B} \sum_{k=1}^B (\log D_\psi(s'_k) - \lambda Q_{\text{shadow}}(s'_k, a_k)). \end{aligned} \quad (3)$$

The first term in \mathcal{L}_G promotes visual imperceptibility, while the second encourages the generator to craft perturbations that minimize the victim’s predicted cumulative reward through the shadow critic, all under a black-box constraint.

3.4. Two-Stage Alternating Optimization

Directly optimizing the generator G_ϕ and the shadow critic Q_{shadow} together often leads to instability, as their objectives

are tightly coupled. To stabilize learning, SEBA adopts a two-stage alternating strategy that separates the updates of the critic and the generator:

Stage 1 (Shadow Model Update). Freeze (G_ϕ, D_ψ) , roll out adversarial interactions to collect tuples (s', a, r, s'_{+1}) , and update Q_{shadow} using the temporal-difference loss in Eq. (2), ensuring that it accurately models the victim’s reward dynamics under perturbations.

Stage 2 (GAN Update). Freeze Q_{shadow} , generate adversarial states s' , obtain corresponding actions a from the victim policy, and update (G_ϕ, D_ψ) according to Eq. (3). This step optimizes the generator for both attack effectiveness and imperceptibility, guided by the stable supervision from the fixed critic.

3.5. World Model for Query Efficiency

To alleviate the cost of querying the real environment, SEBA employs a *world model* \mathcal{W} trained from the replay buffer \mathcal{D} . Following the IRIS framework [22], \mathcal{W} consists of a discrete image tokenizer (E, D) and an autoregressive Transformer \mathcal{G} that predicts future latent tokens and rewards conditioned on past state–action sequences:

$$z_t = E(s_t), \quad (4)$$

$$\hat{z}_{t+1}, \hat{r}_t = \mathcal{G}(z_{\leq t}, a_{\leq t}), \quad (5)$$

$$\hat{s}_{t+1} = D(\hat{z}_{t+1}). \quad (6)$$

World-model training. \mathcal{W} is trained on samples from replay buffer \mathcal{D} to predict next latent tokens and rewards. We use a single joint prediction loss:

$$\begin{aligned} \mathcal{L}_{\mathcal{W}} = & \mathbb{E}_{(s_t, a_t, r_t, s_{t+1}) \sim \mathcal{D}} [-\log p_{\mathcal{G}}(z_{t+1} \mid z_{\leq t}, a_{\leq t})] \\ & + \mathbb{E}_{(s_t, r_t) \sim \mathcal{D}} [\|\hat{r}_t - r_t\|_2^2]. \end{aligned} \quad (7)$$

After $N_{\mathcal{W}}$ training steps, \mathcal{W} is used to generate imagined transitions for SEBA training.

Once trained via Eq. 7, the world model captures visual and reward dynamics, enabling the attacker to generate synthetic transitions $(s'_t, a_t, \hat{r}_t, s'_{t+1})$ without invoking the real environment.

Model-based rollouts. After training, the world model \mathcal{W} is employed to generate *model rollouts*, which simulate transitions for updating both the shadow critic Q_{shadow} and the generator G_ϕ :

$$y_t = \hat{r}_t + \gamma \mathbb{E}_{a \sim \pi(\cdot \mid \hat{s}'_{t+1})} [Q_{\text{shadow}}(\hat{s}'_{t+1}, a)], \quad (8)$$

$$\mathcal{L}_G = -\frac{1}{B} \sum_{k=1}^B (\log D_\psi(\hat{s}'_k) - \lambda Q_{\text{shadow}}(\hat{s}'_k, a_k)). \quad (9)$$

Each real interaction is paired with H model-generated transitions, effectively expanding the replay buffer and reducing real environment queries by $\mathcal{O}(H)$.

Algorithm 1 SEBA: Sample-Efficient Black-box Attack

```

1: Initialize  $G_\phi, D_\psi, Q_{\text{shadow}}, \mathcal{W}$  and buffer  $\mathcal{D} \leftarrow \emptyset$ 
2: Collect real transitions  $(s, a, r, s_{+1})$  and train  $\mathcal{W}$  by
   minimizing  $\mathcal{L}_{\mathcal{W}}$  (Eq. 7)
3: for  $i = 1$  to  $N_{\text{iter}}$  do
4:   Update  $Q_{\text{shadow}}$  (Stage 1, Alg. 2) with TD loss
5:   Update  $(G_\phi, D_\psi)$  (Stage 2, Alg. 3) with fixed  $Q_{\text{shadow}}$ 
6: end for
7: return  $G_\phi$ 

```

Algorithm 2 Stage 1: Train Shadow Critic Q_{shadow}

```

1: // Shadow-critic update loop
2: for  $t = 1$  to  $T_1$  do
3:   Sample  $s_t$  from environment
4:   Compute  $s'_t \leftarrow \text{clip}(s_t + \text{clip}(G_\phi(s_t), -\epsilon, \epsilon), 0, 1)$ 
5:   Obtain action  $a_t \sim \pi(\cdot \mid s'_t)$ 
6:   Step environment to get  $(r_t, s_{t+1}, \text{done}_t)$ 
7:   if use_wm then
8:     Roll out  $\mathcal{W}$  for  $H$  steps from  $s_t$  to produce syn-
       thetic transitions for  $\mathcal{D}$ 
9:   else
10:    Append  $(s'_t, a_t, r_t, s'_{t+1}, \text{done}_t)$  to  $\mathcal{D}$ 
11:   end if
12:   Sample a minibatch from  $\mathcal{D}$ ;
13:   update  $Q_{\text{shadow}}$  by the loss in Eq. (2)
14: end for

```

Algorithm 3 Stage 2: Train (G_ϕ, D_ψ)

```

1: // Generator–discriminator update loop
2: for  $t = 1$  to  $T_2$  do
3:   Sample  $s_t$  from environment or world model  $\mathcal{W}$ 
4:   Compute  $s'_t \leftarrow \text{clip}(s_t + \text{clip}(G_\phi(s_t), -\epsilon, \epsilon), 0, 1)$ 
5:   Obtain action  $a_t \sim \pi(\cdot \mid s'_t)$ 
6:   Update  $(G_\phi, D_\psi)$  using Eq. (3)
7: end for

```

3.6. Overall procedure

Algorithm 1 summarizes SEBA. The world model \mathcal{W} generates synthetic rollouts that are mixed with real transitions in \mathcal{D} for joint updates of Q_{shadow} and G_ϕ . Periodic real-environment queries are interleaved to correct model drift and maintain fidelity. SEBA reuses H synthetic transitions per real step, reducing environment queries by about $1/H$. Final evaluations are performed in the real environment.

4. Experiments

In this section, we present a comprehensive evaluation of SEBA. We consider four aspects: (i) pixel-based MuJoCo control tasks with DrQ-SAC victims, comparing against both 2D image-space attack algorithms and vector-state RL

attack algorithms, evaluated in terms of effectiveness (reward), imperceptibility (FID), and query efficiency (query cost); (ii) transfer to Atari with PPO agents to assess cross-domain generality; (iii) ablations of key components, including the discriminator, the use of noisy states in Stage 1, and the world model; and (iv) targeted attacks on selected action dimensions for fine-grained behavioral control.

4.1. Experimental Setup

Environments and victim agents. We evaluate SEBA on five pixel-based continuous-control tasks from the MuJoCo simulator, which provides diverse physics-based benchmarks for reinforcement learning. Victim agents are trained with DrQ-SAC [7, 30], a variant of SAC that achieves strong performance without auxiliary losses and serves as the basis for many visual RL algorithms [15, 35]. All victim policies are pre-trained and fixed during attack evaluation. Additional results on other visual RL attacks are reported in the Supplementary Material.

Baselines. To our knowledge, we are the first to study *black-box attacks on image-based continuous-control RL agents*. Accordingly, we compare SEBA against two families of baselines: (i) *2D image-space attacks* that directly perturb pixels (PGD [19], C&W [2], SimBA [6], Square [1]); and (ii) *vector-state RL attacker methods* originally developed for low-dimensional observations and adapted here to pixel control (Critic-Based [32], MAD [32], PA-AD [25], OPTIMAL [33]). All baselines are tuned to their best-reported configurations; For fairness, PA-AD and OPTIMAL are adapted to pixel control by using the same generator architecture as SEBA. Implementation details are provided in the Supplementary Material.

Evaluation metrics. We report three metrics:

- (1) **Effectiveness:** cumulative reward (lower is better).
- (2) **Imperceptibility:** measured by the Fréchet Inception Distance (FID) [9] between clean and adversarial state distributions (lower is better).
- (3) **Query efficiency:** we report *Train Env (total)* for total environment queries during attacker training, *Train Vic (total)* for total victim queries during attacker training, and *Atk. Vic (per-step)* for victim queries per step during attack execution. We omit per-step environment queries because they are zero for all methods.

All results are averaged over 10 random seeds and reported as mean \pm standard deviation.

Hyperparameters. SEBA and all baseline methods use the same perturbation bound $\epsilon = 8/255$ for fairness, with $\lambda = 1$ in the generator loss. Key settings include world-model rollout horizon $H = 4$, number of world-model updates $N_w = 200K$, total training iterations $N_{\text{iter}} = 20$, and phase lengths $T_1 = T_2 = 5K$. Additional experiments with varying hyperparameters and other implementation details are reported in the Supplementary Material.

4.2. Pixel-Based MuJoCo Results

Overview. Tables 1–2 summarize the results across five pixel-based MuJoCo tasks. We assess attack performance in terms of reward degradation, perturbation imperceptibility, and query usage.

Effectiveness. We report the cumulative reward of the victim policy under attack. SEBA yields the lowest rewards on all tasks. Representative examples: on *Cheetah Run* SEBA obtains 1.61 ± 3.97 vs. PGD 150.72 ± 49.52 ; on *Reacher Hard* SEBA obtains 0.30 ± 0.90 vs. OPTIMAL 592.64 ± 116.13 . These results show SEBA’s consistent ability to induce long-horizon failures in image-based control.

Imperceptibility. We assess visual subtlety using FID (lower is better). SEBA achieves the lowest FID across all tasks, showing that its perturbations remain closer to the clean observation distribution while still inducing strong performance degradation. Other baselines exhibit noticeably higher FID, reflecting larger visual deviation from clean states.

Query efficiency. SEBA performs attacks with *zero* victim queries at execution time (*Atk. Vic*=0), whereas SimBA and Square require 400 and 202 queries per step, respectively (Table 1). PA-AD and OPTIMAL incur substantially higher training cost, requiring roughly 4M *Env* and *Vic* queries during attacker training, while SEBA uses 160K *Env* and 800K *Vic* queries. This highlights SEBA’s superior sample efficiency and its practicality when both environment interactions and victim queries are limited.

Focused comparison: PA-AD and OPTIMAL. PA-AD [25] and OPTIMAL [33] are the state-of-the-art attacker frameworks in the *vector-state* setting: PA-AD is the strongest *white-box* method, and OPTIMAL is the strongest *black-box* RL-based attacker. Both methods treat the attacker as a policy π_a that generates perturbations δ_t and optimize the long-horizon objective

$$\min_{\pi_a} J(\pi_a) = \mathbb{E} \left[\sum_t -r_t(s_t + \delta_t) \right], \delta_t \sim \pi_a(\cdot | s_t). \quad (10)$$

This formulation is tractable when the observation space is low-dimensional. In pixel-based control, however, the perturbation lies in

$$d = \dim(\delta_t) = 3 \times 84 \times 84 \approx 2 \times 10^4, \quad (11)$$

so the attacker must optimize in an **extremely high-dimensional action space**. This directly leads to: (i) a sharp increase in sample complexity, since exploration in

Table 1. **Image-based attacks on pixel DrQ-SAC agents.** Lower reward and FID indicate stronger attacks. Query cost includes training-time interactions with the environment or victim agent, and attack-time victim queries per step.

Task (Reward ↓)	No Attack	White-box		Black-box		
	Clean	PGD	C&W	SimBA	Square	SEBA
Cheetah Run	859.26 ± 35.00	150.72 ± 49.52	183.41 ± 50.01	52.15 ± 20.09	182.90 ± 23.09	1.61 ± 3.97
Walker Walk	944.28 ± 42.26	342.78 ± 35.82	438.67 ± 28.56	68.77 ± 15.44	752.19 ± 22.22	35.74 ± 6.67
Walker Run	718.15 ± 26.79	118.35 ± 16.38	134.43 ± 25.92	32.87 ± 5.28	258.41 ± 16.31	17.09 ± 4.73
Reacher Hard	870.9 ± 90.43	232.3 ± 31.71	332.0 ± 40.84	2.7 ± 6.60	870.7 ± 90.38	0.3 ± 0.9
Hopper Stand	849.60 ± 128.49	1.85 ± 5.56	8.22 ± 14.61	4.86 ± 6.72	652.10 ± 86.02	1.25 ± 3.75
FID ↓	/	109.43	110.97	78.05	118.01	62.43
Train Env (total) ↓	/	/	/	/	/	160K
Train Vic (total) ↓	/	/	/	/	/	800K
Atk. Vic (per-step) ↓	/	20	20	400	202	0

Table 2. **Vector-state RL attacks adapted to pixel-based control.** Methods originally designed for low-dimensional vector observations degrade in high-dimensional image space, while SEBA remains both effective and query-efficient.

Task (Reward ↓)	No Attack	White-box			Black-box	
	Clean	Critic-Based	MAD	PA-AD	OPTIMAL	SEBA
Cheetah Run	859.26 ± 35.00	117.86 ± 39.44	29.02 ± 11.42	146.61 ± 24.44	271.73 ± 34.72	1.61 ± 3.97
Walker Walk	944.28 ± 42.26	231.03 ± 99.92	149.58 ± 43.54	323.96 ± 51.72	631.30 ± 138.28	35.74 ± 6.67
Walker Run	718.15 ± 26.79	117.42 ± 16.26	38.63 ± 4.58	186.15 ± 13.54	325.86 ± 15.69	17.09 ± 4.73
Reacher Hard	870.9 ± 90.43	213.6 ± 72.99	26.19 ± 16.5	45.37 ± 28.44	592.64 ± 116.13	0.3 ± 0.9
Hopper Stand	849.60 ± 128.49	8.50 ± 17.11	1.32 ± 3.97	25.02 ± 5.99	331.91 ± 68.83	1.25 ± 3.75
FID ↓	/	115.46	106.34	97.55	93.04	62.43
Train Env (total) ↓	/	/	/	4M	4M	160K
Train Vic (total) ↓	/	/	/	4M	4M	800K
Atk. Vic (per-step) ↓	/	20	11	0	0	0

\mathbb{R}^d becomes inefficient; and (ii) weak, noisy gradient signals, making policy optimization unstable or ineffective.

In contrast, SEBA does not learn a policy in this high-dimensional perturbation space. Instead, it directly trains a generator G_ϕ guided by the shadow critic:

$$\delta_t = G_\phi(s_t), \nabla_\phi \mathcal{L}_G = -\nabla_\phi Q_{\text{shadow}}(s_t + \delta_t, a_t), \quad (12)$$

so optimization focuses only on perturbations that directly reduce value, without requiring RL-based exploration over \mathbb{R}^d . This allows SEBA to remain effective in pixel space while PA-AD and OPTIMAL degrade significantly (Table 2).

4.3. Atari Experiments

Table 3 evaluates SEBA on three Atari games (Freeway, Pong, Alien) using *Rainbow* as the victim agent. The state space remains pixel-based as in MuJoCo, but the action space in Atari is *discrete* rather than continuous. This setting tests whether SEBA can still shape behavior when ac-

tions are selected from a finite action set.

SEBA consistently reduces reward across all three games. For example, on *Freeway* the reward decreases from 34 → 10, and on *Alien* from 8858 → 982. SEBA outperforms both white-box Critic-Based [32] and MAD [32], as well as the black-box OPTIMAL [33] baseline. Although **PA-AD** [25] achieves the strongest overall degradation due to full gradient access, such white-box information is not available in black-box threat models.

SEBA also achieves the lowest FID (81.7), indicating that its perturbed observations remain visually close to the clean states.

In terms of query cost, PA-AD and OPTIMAL require 2M environment interactions and 2M victim queries during training, whereas SEBA trains with a fixed budget of 80K environment queries and 400K victim queries and requires *zero* victim access at attack time. This makes SEBA more practical in scenarios where interaction with either the environment or the victim policy is restricted or expensive.

Table 3. **Attacks on pixel-based Atari Rainbow agents.** Lower reward and FID indicate stronger attacks; query rows report training-time ENV/VIC queries and attack-time victim queries per step.

Task (Reward ↓)	No Attack	White-box			Black-box	
	Clean	Critic-Based	MAD	PA-AD	OPTIMAL	SEBA
Freeway	34 \pm 1	24 \pm 0	21 \pm 4	6\pm3	32 \pm 5	10\pm4
Pong	21 \pm 0	14 \pm 4	15 \pm 1	-21\pm0	18 \pm 2	3\pm0
Alien	8858 \pm 1007	3911 \pm 502	3364 \pm 698	443\pm281	7400 \pm 1623	982\pm542
FID ↓	/	131.6	136.4	102.4	113.9	81.7
Train Env (total) ↓	/	/	/	2M	2M	80K
Train Vic (total) ↓	/	/	/	2M	2M	400K
Atk. Vic (per-step) ↓	/	20	11	0	0	0

Overall, these Atari results show that SEBA generalizes beyond continuous control and remains effective in pixel-based discrete-action settings.

4.4. Ablation Study

To assess the contribution of each component in SEBA, we evaluate three ablated variants: **(-D)** removes the discriminator in Stage 2; **(-Noise)** replaces the perturbed states in Stage 1 with clean states (i.e., training uses s_t rather than $s_t + \epsilon$); and **(-WM)** removes the world model, training the critic solely from real environment rollouts. All other training settings and hyperparameters are kept identical across variants. Quantitative results are summarized in Table 4.

Discriminator. Removing the discriminator **(-D)** leads to a large increase in FID (from 62.43 to 97.18), showing that the perturbations are visually less consistent with clean observations. The change in reward is much smaller, meaning that the discriminator is not the main source of attack effectiveness. Its primary role is to stabilize the generator so that perturbations remain visually smooth, while the performance degradation is still mainly driven by the shadow critic.

Stage 1 Perturbed States. Replacing perturbed states with clean states **(-Noise)** yields the largest performance drop (e.g., Walker Walk: 35.74 \rightarrow 118.11). In Stage 1, the shadow critic is trained on perturbed states $s'_t = s_t + G_\phi(s_t)$, so that the TD targets in Eq. (2) reflect the cumulative rewards the agent obtains under perturbations. This alignment ensures that Q_{shadow} provides meaningful gradients to guide G_ϕ .

When clean states are used instead, the critic is learned under a mismatched state distribution, making its value estimates less reliable under perturbations, which in turn leads to substantially weaker attacks in **(-Noise)**.

World Model. Removing the world model **(-WM)** yields comparable or slightly higher attack strength, but increases environment queries from 160K to 800K. The world model does not directly boost attack performance; instead, it enhances sample efficiency by generating synthetic transitions for updating both the shadow critic and the generator.

Summary. The three components serve complementary purposes: the discriminator stabilizes visual appearance, Stage 1 perturbed states ensure the critic remains reliable under the perturbed environment, and the world model reduces environment query cost. Together, these components yield a method that is both effective and efficient.

4.5. Targeted Attack Evaluation

We evaluate whether SEBA can be adapted to achieve *targeted* control. The victim’s action space is $[-1.0, 1.0]^m$; we therefore select a target sub-interval $\mathcal{R}_{\text{target}} \subset [-1.0, 1.0]$ for a single action dimension i . An attack is counted as successful if the victim’s executed action satisfies $a_t^{(i)} \in \mathcal{R}_{\text{target}}$. We report the success rate over full evaluation episodes to obtain per-task performance statistics.

Setup. To adapt SEBA for targeted control, we adopt the training structure in Eq. (3) and modify only the generator objective to encourage the victim’s chosen action dimension i to fall within the target interval $\mathcal{R}_{\text{target}} \subset [-1, 1]$. The modified part of the generator loss is given by:

$$\max_{\phi} Q_{\text{shadow}}(s_t + G_{\phi}(s_t), a_t) \quad \text{s.t.} \quad a_t^{(i)} \in \mathcal{R}_{\text{target}}. \quad (13)$$

Here, a_t denotes the victim’s action under the perturbed observation $s_t + G_{\phi}(s_t)$. This adjustment encourages the generator to produce perturbations that steer the selected action dimension into the target interval, while still maintaining visually subtle modifications consistent with the discriminator constraint.

Table 4. **Ablation study on SEBA components.** Each variant removes one module: **(-D)** removes the discriminator, **(-Noise)** replaces noisy perturbed states in Stage 1 with clean states. and **(-WM)** removes the world model. Lower reward and FID indicate stronger attacks.

Task (Reward ↓)	Clean	SEBA	(-D)	(-Noise)	(-WM)
Cheetah Run	859.26 \pm 35.00	1.61 \pm 3.97	3.15 \pm 5.24	19.25 \pm 9.31	0.18 \pm 0.04
Walker Walk	944.28 \pm 42.26	35.74 \pm 6.67	22.64 \pm 8.13	118.11 \pm 27.64	36.01 \pm 10.54
Walker Run	718.15 \pm 26.79	17.09 \pm 4.73	22.44 \pm 2.54	60.27 \pm 11.23	28.04 \pm 14.98
Reacher Hard	870.90 \pm 90.43	0.30 \pm 0.90	0.33 \pm 0.14	12.98 \pm 9.21	0.00 \pm 0.00
Hopper Stand	849.60 \pm 128.49	1.25 \pm 3.75	3.10 \pm 2.89	10.78 \pm 13.18	0.35 \pm 0.49
FID ↓	/	62.43	97.18	60.72	63.98
Train Env (total) ↓	/	160K	160K	160K	800K
Train Vic (total) ↓	/	800K	800K	800K	800K

Table 5. **Targeted attack success rates (%)**: an attack is counted as success if the selected action dimension $a_t^{(i)}$ falls within the target range $\mathcal{R}_{\text{target}} \subset [-1, 1]$.

Task	Selected Dimension	Target Range	PGD (%) ↑	Critic-Based (%) ↑	SEBA (%) ↑
Cheetah Run	4 of 6	[0.3, 0.5]	60.8	68.1	96.6
Walker Walk	5 of 6	[-0.6, -0.4]	37.2	53.2	91.3
Walker Run	2 of 6	[-0.7, -0.5]	58.0	64.5	95.6
Reacher Hard	2 of 2	[0.0, 0.2]	46.2	57.4	93.2
Hopper Stand	3 of 4	[0.6, 0.8]	76.6	84.5	98.8

Results and discussion. Table 5 shows that SEBA attains substantially higher targeted-success rates than PGD and the Critic-Based attacker across all tasks. For example, on *Walker Walk* SEBA achieves **91.3%** success versus 37.2% (PGD) and 53.2% (Critic-Based); on *Reacher Hard* SEBA reaches **93.2%** compared to 46.2% and 57.4%. These results indicate that SEBA can not only degrade overall performance but also steer specific action components toward desired target ranges. This demonstrates that the perturbations are not only disruptive but can be shaped to enforce fine-grained control behavior when required.

5. Conclusion

This work presented **SEBA**, a sample-efficient framework for black-box adversarial attacks on visual reinforcement learning agents. By combining a shadow critic, a GAN-based perturbation generator, and a learned world model, SEBA enables strong attacks without access to gradients or internal model parameters. Experiments on pixel-based MuJoCo and Atari benchmarks show that SEBA achieves superior performance in terms of reward degradation, visual imperceptibility, and query efficiency, outperforming both white-box and black-box baselines. Moreover, SEBA extends naturally to targeted control tasks, demonstrating flexible and transferable attack capability across visual RL domains. These results highlight SEBA as a practical and effective approach for evaluating the robustness of embodied AI systems under limited-access conditions.

References

- [1] Maksym Andriushchenko, Francesco Croce, Nicolas Flammarion, and Matthias Hein. Square attack: A query-efficient black-box adversarial attack via random search. In *Computer Vision - ECCV 2020 - 16th European Conference, Glasgow, UK, August 23-28, 2020, Proceedings, Part XXIII*, pages 484–501. Springer, 2020. 5
- [2] Nicholas Carlini and David A. Wagner. Towards evaluating the robustness of neural networks. In *2017 IEEE Symposium on Security and Privacy, SP 2017, San Jose, CA, USA, May 22-26, 2017*, pages 39–57. IEEE Computer Society, 2017. 5
- [3] Edoardo Cetin, Philip J. Ball, Stephen J. Roberts, and Oya Çeliktutan. Stabilizing off-policy deep reinforcement learning from pixels. In *International Conference on Machine Learning, ICML 2022, 17-23 July 2022, Baltimore, Maryland, USA*, pages 2784–2810. PMLR, 2022. 2
- [4] Hyesong Choi, Hunsang Lee, Wonil Song, Sangryul Jeon, Kwanghoon Sohn, and Dongbo Min. Local-guided global: Paired similarity representation for visual reinforcement learning. In *IEEE/CVF Conference on Computer Vision and Pattern Recognition, CVPR 2023, Vancouver, BC, Canada, June 17-24, 2023*, pages 15072–15082. IEEE, 2023. 1
- [5] Carles Gelada, Saurabh Kumar, Jacob Buckman, Ofir Nachum, and Marc G. Bellemare. Deepmdp: Learning continuous latent space models for representation learning. In *Proceedings of the 36th International Conference on Machine Learning, ICML 2019, 9-15 June 2019, Long Beach, California, USA*, pages 2170–2179. PMLR, 2019. 2
- [6] Chuan Guo, Jacob R. Gardner, Yurong You, Andrew Gordon Wilson, and Kilian Q. Weinberger. Simple black-box adver-

- sarial attacks. In *Proceedings of the 36th International Conference on Machine Learning, ICML 2019, 9-15 June 2019, Long Beach, California, USA*, pages 2484–2493. PMLR, 2019. 5
- [7] Tuomas Haarnoja, Aurick Zhou, Pieter Abbeel, and Sergey Levine. Soft actor-critic: Off-policy maximum entropy deep reinforcement learning with a stochastic actor. In *Proceedings of the 35th International Conference on Machine Learning, ICML 2018, Stockholmsmässan, Stockholm, Sweden, July 10-15, 2018*, pages 1856–1865. PMLR, 2018. 5
- [8] Danijar Hafner, Timothy P. Lillicrap, Jimmy Ba, and Mohammad Norouzi. Dream to control: Learning behaviors by latent imagination. In *8th International Conference on Learning Representations, ICLR 2020, Addis Ababa, Ethiopia, April 26-30, 2020*. OpenReview.net, 2020. 2
- [9] Martin Heusel, Hubert Ramsauer, Thomas Unterthiner, Bernhard Nessler, and Sepp Hochreiter. Gans trained by a two time-scale update rule converge to a local nash equilibrium. In *Advances in Neural Information Processing Systems 30: Annual Conference on Neural Information Processing Systems 2017, December 4-9, 2017, Long Beach, CA, USA*, pages 6626–6637, 2017. 5
- [10] Sandy H. Huang, Nicolas Papernot, Ian J. Goodfellow, Yan Duan, and Pieter Abbeel. Adversarial attacks on neural network policies. In *5th International Conference on Learning Representations, ICLR 2017, Toulon, France, April 24-26, 2017, Workshop Track Proceedings*. OpenReview.net, 2017. 1
- [11] Ezgi Korkmaz. Nesterov momentum adversarial perturbations in the deep reinforcement learning domain. In *International Conference on Machine Learning, ICML, 2020*.
- [12] Ezgi Korkmaz. Deep reinforcement learning policies learn shared adversarial features across mdps. In *Thirty-Sixth AAAI Conference on Artificial Intelligence, AAAI 2022, Thirty-Fourth Conference on Innovative Applications of Artificial Intelligence, IAAI 2022, The Twelveth Symposium on Educational Advances in Artificial Intelligence, EAAI 2022 Virtual Event, February 22 - March 1, 2022*, pages 7229–7238. AAAI Press, 2022.
- [13] Ezgi Korkmaz. Adversarial robust deep reinforcement learning requires redefining robustness. In *Thirty-Seventh AAAI Conference on Artificial Intelligence, AAAI 2023, Thirty-Fifth Conference on Innovative Applications of Artificial Intelligence, IAAI 2023, Thirteenth Symposium on Educational Advances in Artificial Intelligence, EAAI 2023, Washington, DC, USA, February 7-14, 2023*, pages 8369–8377. AAAI Press, 2023. 1
- [14] Michael Laskin, Aravind Srinivas, and Pieter Abbeel. CURL: contrastive unsupervised representations for reinforcement learning. In *Proceedings of the 37th International Conference on Machine Learning, ICML 2020, 13-18 July 2020, Virtual Event*, pages 5639–5650. PMLR, 2020. 2
- [15] Kuang-Huei Lee, Ian Fischer, Anthony Z. Liu, Yijie Guo, Honglak Lee, John F. Canny, and Sergio Guadarrama. Predictive information accelerates learning in RL. In *Advances in Neural Information Processing Systems 33: Annual Conference on Neural Information Processing Systems 2020, NeurIPS 2020, December 6-12, 2020, virtual*, 2020. 5
- [16] Jiashun Liu, Jianye Hao, Xiaotian Hao, Yi Ma, Yan Zheng, Yujing Hu, and Tangjie Lv. Unlock the intermittent control ability of model free reinforcement learning. In *Advances in Neural Information Processing Systems 38: Annual Conference on Neural Information Processing Systems 2024, NeurIPS 2024, Vancouver, BC, Canada, December 10 - 15, 2024*, 2024. 1
- [17] Zuxin Liu, Zijian Guo, Zhepeng Cen, Huan Zhang, Jie Tan, Bo Li, and Ding Zhao. On the robustness of safe reinforcement learning under observational perturbations. In *The Eleventh International Conference on Learning Representations, ICLR 2023, Kigali, Rwanda, May 1-5, 2023*. OpenReview.net, 2023. 2
- [18] Vinu Maddumage, Sarath Kodagoda, Marc G. Carmichael, Amal Gunatilake, Karthick Thiagarajan, and Jodi Martin. Relative velocity-based reward model for socially-aware navigation with deep reinforcement learning. In *IEEE International Conference on Robotics and Automation, ICRA 2025, Atlanta, GA, USA, May 19-23, 2025*, pages 10448–10454. IEEE, 2025. 1
- [19] Aleksander Madry, Aleksandar Makelov, Ludwig Schmidt, Dimitris Tsipras, and Adrian Vladu. Towards deep learning models resistant to adversarial attacks. In *6th International Conference on Learning Representations, ICLR 2018, Vancouver, BC, Canada, April 30 - May 3, 2018, Conference Track Proceedings*. OpenReview.net, 2018. 5
- [20] Jeremy McMahan, Young Wu, Xiaojin Zhu, and Qiaomin Xie. Optimal attack and defense for reinforcement learning. In *Thirty-Eighth AAAI Conference on Artificial Intelligence, AAAI 2024, Thirty-Sixth Conference on Innovative Applications of Artificial Intelligence, IAAI 2024, Fourteenth Symposium on Educational Advances in Artificial Intelligence, EAAI 2024, February 20-27, 2024, Vancouver, Canada*, pages 14332–14340. AAAI Press, 2024. 2
- [21] Shaunak A. Mehta, Soheil Habibi, and Dylan P. Losey. Waypoint-based reinforcement learning for robot manipulation tasks. In *IEEE/RSJ International Conference on Intelligent Robots and Systems, IROS 2024, Abu Dhabi, United Arab Emirates, October 14-18, 2024*, pages 541–548. IEEE, 2024. 1
- [22] Vincent Micheli, Eloi Alonso, and François Fleuret. Transformers are sample-efficient world models. In *The Eleventh International Conference on Learning Representations, ICLR 2023, Kigali, Rwanda, May 1-5, 2023*. OpenReview.net, 2023. 2, 4
- [23] Volodymyr Mnih, Koray Kavukcuoglu, David Silver, Andrei A. Rusu, Joel Veness, Marc G. Bellemare, Alex Graves, Martin A. Riedmiller, Andreas Fidjeland, Georg Ostrovski, Stig Petersen, Charles Beattie, Amir Sadik, Ioannis Antonoglou, Helen King, Dharmashan Kumaran, Daan Wierstra, Shane Legg, and Demis Hassabis. Human-level control through deep reinforcement learning. *Nat.*, 518(7540):529–533, 2015. 1
- [24] Anay Pattanaik, Zhenyi Tang, Shuijing Liu, Gautham Bommannan, and Girish Chowdhary. Robust deep reinforcement learning with adversarial attacks. In *Proceedings of the 17th International Conference on Autonomous Agents and Multi-Agent Systems, AAMAS 2018, Stockholm, Sweden, July 10-*

- 15, 2018, pages 2040–2042. International Foundation for Autonomous Agents and Multiagent Systems Richland, SC, USA / ACM, 2018. [2](#)
- [25] Yanchao Sun, Ruijie Zheng, Yongyuan Liang, and Furong Huang. Who is the strongest enemy? towards optimal and efficient evasion attacks in deep RL. In *The Tenth International Conference on Learning Representations, ICLR 2022, Virtual Event, April 25-29, 2022*. OpenReview.net, 2022. [1](#), [2](#), [5](#), [6](#)
- [26] Yunhao Tang, Zhaohan Daniel Guo, Pierre Harvey Richemond, Bernardo Ávila Pires, Yash Chandak, Rémi Munos, Mark Rowland, Mohammad Gheshlaghi Azar, Charline Le Lan, Clare Lyle, András György, Shantanu Thakoor, Will Dabney, Bilal Piot, Daniele Calandriello, and Michal Valko. Understanding self-predictive learning for reinforcement learning. In *International Conference on Machine Learning, ICML 2023, 23-29 July 2023, Honolulu, Hawaii, USA*, pages 33632–33656. PMLR, 2023. [2](#)
- [27] Hado van Hasselt, Arthur Guez, and David Silver. Deep reinforcement learning with double q-learning. In *Proceedings of the Thirtieth AAAI Conference on Artificial Intelligence, February 12-17, 2016, Phoenix, Arizona, USA*, pages 2094–2100. AAAI Press, 2016. [1](#)
- [28] Haoran Xu, Peixi Peng, Guang Tan, Yuan Li, Xinhai Xu, and Yonghong Tian. DMR: decomposed multi-modality representations for frames and events fusion in visual reinforcement learning. In *IEEE/CVF Conference on Computer Vision and Pattern Recognition, CVPR 2024, Seattle, WA, USA, June 16-22, 2024*, pages 26498–26508. IEEE, 2024. [1](#)
- [29] Shojiro Yamabe, Kazuto Fukuchi, Ryoma Senda, and Jun Sakuma. Behavior-targeted attack on reinforcement learning with limited access to victim’s policy. *CoRR*, abs/2406.03862, 2024. [2](#)
- [30] Denis Yarats, Ilya Kostrikov, and Rob Fergus. Image augmentation is all you need: Regularizing deep reinforcement learning from pixels. In *9th International Conference on Learning Representations, ICLR 2021, Virtual Event, Austria, May 3-7, 2021*. OpenReview.net, 2021. [2](#), [5](#)
- [31] Denis Yarats, Amy Zhang, Ilya Kostrikov, Brandon Amos, Joelle Pineau, and Rob Fergus. Improving sample efficiency in model-free reinforcement learning from images. In *Thirty-Fifth AAAI Conference on Artificial Intelligence, AAAI 2021, Thirty-Third Conference on Innovative Applications of Artificial Intelligence, IAAI 2021, The Eleventh Symposium on Educational Advances in Artificial Intelligence, EAAI 2021, Virtual Event, February 2-9, 2021*, pages 10674–10681. AAAI Press, 2021. [2](#)
- [32] Huan Zhang, Hongge Chen, Chaowei Xiao, Bo Li, Mingyan Liu, Duane S. Boning, and Cho-Jui Hsieh. Robust deep reinforcement learning against adversarial perturbations on state observations. In *Advances in Neural Information Processing Systems 33: Annual Conference on Neural Information Processing Systems 2020, NeurIPS 2020, December 6-12, 2020, virtual*, 2020. [1](#), [2](#), [5](#), [6](#)
- [33] Huan Zhang, Hongge Chen, Duane S. Boning, and Cho-Jui Hsieh. Robust reinforcement learning on state observations with learned optimal adversary. In *9th International Conference on Learning Representations, ICLR 2021, Virtual Event, Austria, May 3-7, 2021*. OpenReview.net, 2021. [1](#), [2](#), [5](#), [6](#)
- [34] Hongming Zhang, Tongzheng Ren, Chenjun Xiao, Dale Schuurmans, and Bo Dai. Provable representation with efficient planning for partially observable reinforcement learning. In *Forty-first International Conference on Machine Learning, ICML 2024, Vienna, Austria, July 21-27, 2024*. OpenReview.net, 2024. [2](#)
- [35] Renzhe Zhou, Chenxiao Gao, Zongzhang Zhang, and Yang Yu. Generalizable task representation learning for offline meta-reinforcement learning with data limitations. In *Thirty-Eighth AAAI Conference on Artificial Intelligence, AAAI 2024, Thirty-Sixth Conference on Innovative Applications of Artificial Intelligence, IAAI 2024, Fourteenth Symposium on Educational Advances in Artificial Intelligence, EAAI 2024, February 20-27, 2024, Vancouver, Canada*, pages 17132–17140. AAAI Press, 2024. [5](#)